

$B_{(s)} \rightarrow D_{(s)}$ semileptonic decays with NRQCD-HISQ valence quarks

Christopher J. Monahan*

New High Energy Theory Center and Department of Physics and Astronomy, Rutgers, The State University of New Jersey, 136 Frelinghuysen Road, Piscataway, NJ 08854, USA
E-mail: chris.monahan@rutgers.edu

Heechang Na

Ohio Supercomputer Center, 1224 Kinnear Road, Columbus, OH 43212, USA
Department of Physics and Astronomy, University of Utah, Salt Lake City, UT 84112, USA

Chris M. Bouchard

School of Physics and Astronomy, University of Glasgow, Glasgow G12 8QQ, UK
Department of Physics and Astronomy, College of William and Mary, Williamsburg, VA 23187, USA

G. Peter Lepage

Laboratory of Elementary Particle Physics, Cornell University, Ithaca, NY 14853, USA

Junko Shigemitsu

Department of Physics, The Ohio State University, Columbus, OH 43210, USA

We present a calculation of the form factors, f_0 and f_+ , for the $B_{(s)} \rightarrow D_{(s)}$ semileptonic decays. Our work uses the MILC $n_f = 2 + 1$ AsqTad configurations with NRQCD and HISQ valence quarks at four values of the momentum transfer q^2 . We provide results for the chiral-continuum extrapolations of the scalar and vector form factors.

34th annual International Symposium on Lattice Field Theory
24-30 July 2016
University of Southampton, UK

*Speaker.

1. Introduction

Precision measurements of B and B_s meson decays at the Large Hadron Collider are an important tool in the search for new physics. For example, the first observation of the rare decay $B_s \rightarrow \mu^+ \mu^-$, through a combined analysis by the LHCb and CMS collaborations [1], tested the Standard Model prediction of the branching fraction. In the Standard Model this decay is doubly-suppressed, but the branching fraction may receive large contributions from new physics effects. Currently, the measured branching fraction is consistent with Standard Model expectations, but there is still room for new physics, given the experimental and theoretical uncertainties. Run II at the LHC should significantly reduce experimental uncertainties for a wide range of $B_{(s)}$ decays. Tightening constraints on potential new physics therefore requires a similar improvement in the theoretical determination of the Standard Model expectations.

The B_s meson branching fraction $\mathcal{B}(B_s \rightarrow \mu^+ \mu^-)$ can be expressed in terms of the ratio of fragmentation fractions, f_d/f_s . The fragmentation fraction f_q gives the probability that a b -quark hadronizes into a B_q meson. Reducing sources of systematic uncertainties in the value of this ratio will improve not just the precision of the determination of the $B_s \rightarrow \mu^+ \mu^-$ branching fraction, but a range of other B_s meson decay branching fractions at the LHC as well [2].

The ratio of the fragmentation fractions, f_d/f_s , can be extracted from the ratio of the scalar form factors of the $B \rightarrow D\ell\nu$ and $B_s \rightarrow D_s\ell\nu$ semileptonic decays [3]. There is currently only one lattice determination of the form factor ratio, using heavy clover bottom and charm quarks [4]. The form factors, $f_+(q^2)$ and $f_0(q^2)$, for the semileptonic decay $B_s \rightarrow D_s\ell\nu$ were determined with twisted mass fermions for the region near zero recoil in [5].

In addition to determining the fragmentation ratio relevant to the measurement of the branching fraction for the rare decay, $B_s \rightarrow \mu^+ \mu^-$, the semileptonic $B_s \rightarrow D_s\ell\nu$ decay provides a new method to determine the CKM matrix element $|V_{cb}|$. There is a long-standing tension between determinations of $|V_{cb}|$ from exclusive and inclusive measurements of the semileptonic B meson decays (see, for example, [6]), although recent analyses suggest the tension has eased [7]. Future experimental observation of the $B_s \rightarrow D_s\ell\nu$ decay, combined with lattice predictions of the form factors, may shed light on the V_{cb} puzzle.

We report on the HPQCD collaboration's calculations of the form factors, $f_+(q^2)$ and $f_0(q^2)$, for the semileptonic decays $B_{(s)} \rightarrow D_{(s)}\ell\nu$, using the non-relativistic (NRQCD) action for the bottom quarks and the Highly Improved Staggered Quark (HISQ) action for the charm quarks. Our results for the $B \rightarrow D\ell\nu$ decay appeared first in [8]. We refer the reader to Sections II and III of [8] for further details of the analysis.

2. Ensemble details

We use five gauge ensembles, summarized in Table 1, generated by the MILC collaboration [9]. These ensembles include three “coarse” (with lattice spacing $a \approx 0.12$ fm) and two “fine” (with $a \approx 0.09$ fm) ensembles, incorporating $n_f = 2 + 1$ flavors of AsqTad sea quarks.

We study $B_{(s)} \rightarrow D_{(s)}$ semileptonic decays by evaluating the matrix element of the bottom-charm vector current, V^μ , between $B_{(s)}$ and $D_{(s)}$ states. We express these matrix elements in terms

Table 1: Simulation details on three ‘‘coarse’’ and two ‘‘fine’’ $n_f = 2 + 1$ MILC ensembles.

Set	r_1/a	m_l/m_s (sea)	N_{conf}	N_{tsrc}	$L^3 \times N_t$	am_b	am_s	am_c	$aE_{b\bar{b}}^{\text{sim}}$
C1	2.647	0.005/0.050	2096	4	$24^3 \times 64$	2.650	0.0489	0.6207	0.28356(15)
C2	2.618	0.010/0.050	2256	2	$20^3 \times 64$	2.688	0.0492	0.6300	0.28323(18)
C3	2.644	0.020/0.050	1200	2	$20^3 \times 64$	2.650	0.0491	0.6235	0.27897(20)
F1	3.699	0.0062/0.031	1896	4	$28^3 \times 96$	1.832	0.0337	0.4130	0.25653(14)
F2	3.712	0.0124/0.031	1200	4	$28^3 \times 96$	1.826	0.0336	0.4120	0.25558(28)

of the form factors $f_+^{(s)}(q^2)$ and $f_0^{(s)}(q^2)$ as

$$\langle D_{(s)}(p_{D_{(s)}}) | V^\mu | B_{(s)}(p_{B_{(s)}}) \rangle = f_0^{(s)}(q^2) \frac{M_{B_{(s)}}^2 - M_{D_{(s)}}^2}{q^2} q^\mu + f_+^{(s)}(q^2) \left[p_{B_{(s)}}^\mu + p_{D_{(s)}}^\mu - \frac{M_{B_{(s)}}^2 - M_{D_{(s)}}^2}{q^2} q^\mu \right], \quad (2.1)$$

where the momentum transfer is $q^\mu = p_{B_{(s)}}^\mu - p_{D_{(s)}}^\mu$. In practice it is simpler to work with the form factors $f_{\parallel}^{(s)}$ and $f_{\perp}^{(s)}$, which are related to $f_+^{(s)}(q^2)$ and $f_0^{(s)}(q^2)$ via

$$f_+^{(s)}(q^2) = \frac{1}{\sqrt{2M_{B_{(s)}}}} \left[f_{\parallel}^{(s)}(q^2) + (M_{B_{(s)}} - E_{D_{(s)}}) f_{\perp}^{(s)}(q^2) \right], \quad (2.2)$$

$$f_0^{(s)}(q^2) = \frac{\sqrt{2M_{B_{(s)}}}}{M_{B_{(s)}}^2 - M_{D_{(s)}}^2} \left[(M_{B_{(s)}} - E_{D_{(s)}}) f_{\parallel}^{(s)}(q^2) + (E_{D_{(s)}}^2 - M_{D_{(s)}}^2) f_{\perp}^{(s)}(q^2) \right]. \quad (2.3)$$

Here $E_{D_{(s)}}$ is the energy of the daughter $D_{(s)}$ meson in the rest frame of the $B_{(s)}$ meson.

We calculate $B_{(s)}$ and $D_{(s)}$ meson two-point correlators and three-point correlators of the bottom-charm currents, J_μ . We use smeared heavy-light or heavy-strange bilinears to represent the $B_{(s)}$ meson, with either delta-function or Gaussian smearing. Three-point correlators are computed as follows: The $B_{(s)}$ meson is created at time t_0 ; a current J_μ inserted at timeslice t ; and the $D_{(s)}$ meson annihilated at timeslice $t_0 + T$, where $t_0 < t < t_0 + T$. We use four values of T and generate data for four values of the $D_{(s)}$ meson momenta, $\vec{p}_{D_{(s)}} \in 2\pi/(aL)\{(0,0,0), (1,0,0), (1,1,0), (1,1,1)\}$, where L is the spatial lattice extent. We work in the rest frame of the $B_{(s)}$ meson.

We match the NRQCD-HISQ currents, J_μ , at one loop in perturbation theory, that is, through $\mathcal{O}(\alpha_s, \Lambda_{\text{QCD}}/m_b, \alpha_s/am_b)$, where am_b is the bare lattice mass [10]. We re-scale all currents by the tree-level massive wave function renormalization for the HISQ charm quarks [8].

3. Correlator fits

We fit $B_{(s)}$ and $D_{(s)}$ meson two-point functions to a sum of decaying exponentials in Euclidean

time, t ,

$$C_{B_{(s)}}^{\beta,\alpha}(t) = \sum_{i=0}^{N_{B_{(s)}}-1} b_i^\beta b_i^{\alpha*} e^{-E_i^{B_{(s)},\text{sim}} t} + \sum_{i=0}^{N'_{B_{(s)}}-1} b_i'^\beta b_i'^{\alpha*} (-1)^t e^{-E_i'^{B_{(s)},\text{sim}} t}, \quad (3.1)$$

$$C_{D_{(s)}}(t; \vec{p}) = \sum_{i=0}^{N_{D_{(s)}}-1} |d_i|^2 \left[e^{-E_i^{D_{(s)}} t} + e^{-E_i^{D_{(s)}} (N_t-t)} \right] + \sum_{i=0}^{N'_{D_{(s)}}-1} |d_i'|^2 (-1)^t \left[e^{-E_i'^{D_{(s)}} t} + e^{-E_i'^{D_{(s)}} (N_t-t)} \right] \quad (3.2)$$

The superscripts α and β indicate the two forms of smearing for the $B_{(s)}$ meson source (delta function or Gaussian). The amplitudes associated with the ordinary and oscillatory states are b_i and b_i' , with associated meson energies $E_i^{B_{(s)},\text{sim}}$ and $E_i'^{B_{(s)},\text{sim}}$, and d_i and d_i' , where the corresponding meson energies are $E_i^{D_{(s)}}$ and $E_i'^{D_{(s)}}$, respectively. The ground state $B_{(s)}$ energy in NRQCD, $E_0^{B_{(s)},\text{sim}}$, is not equal to the true energy in full QCD, $E_0^{B_{(s)}}$, because the b -quark rest mass has been integrated out in NRQCD. Here $\overline{M}_{b\bar{b}}^{\text{exp}}$ is the spin-averaged Υ mass used to tune the b -quark mass and $aE_{b\bar{b}}^{\text{sim}}$ was determined in [11]. For both $B_{(s)}$ and $D_{(s)}$ two-point functions, N is the number of exponentials included in the fit.

For the three-point correlator, we use an ansatz that incorporates four terms, each of which is a sum of exponentials, similar to the two-point forms shown above. For the full form, see [8]. We then determine the hadronic matrix element between $B_{(s)}$ and $D_{(s)}$, in the rest frame of the $B_{(s)}$ meson, from

$$\langle D_{(s)}(p) | V^\mu | B_{(s)} \rangle = \frac{A_{00}^\alpha}{d_0 b_0^{\alpha*}} \sqrt{2a^3 E_0^{D_{(s)}}} \sqrt{2a^3 M_{B_{(s)}}}. \quad (3.3)$$

We fit these correlators using Bayesian multi-exponential fitting python packages `lsqfit` and `corrfitter` [12], an approach that has been used by the HPQCD collaboration for a wide range of lattice calculations.

We tested a number of indicators of fit stability, consistency, and goodness-of-fit to check the fit results. For example, we checked that, beyond a minimum number of exponentials, the fit results are independent of the number of exponentials included in the fit. We tested three types of fits: simultaneous fits to correlator data for all four spatial momenta; chained fits (discussed in detail in the appendices of [13]) to correlator data for all four spatial momenta simultaneously; and “individual” fits, including the correlator data for just a single daughter meson momentum in each fit. All three fit approaches give consistent results.

The simultaneous fits, with or without chaining, have the advantage that they capture the correlations between momenta, which is then reflected in the uncertainty quoted in the fit results. The chained fits give slightly better values of reduced χ^2 and are about ten percent faster than the simultaneous fits, which is an important consideration for the large three-point fits. We take the result for $N_{\text{exp}} = 5$ from the chained fit as our final result for each momentum. Choosing to use chained fits for both two- and three-point fits ensures a consistent approach throughout the fitting procedure.

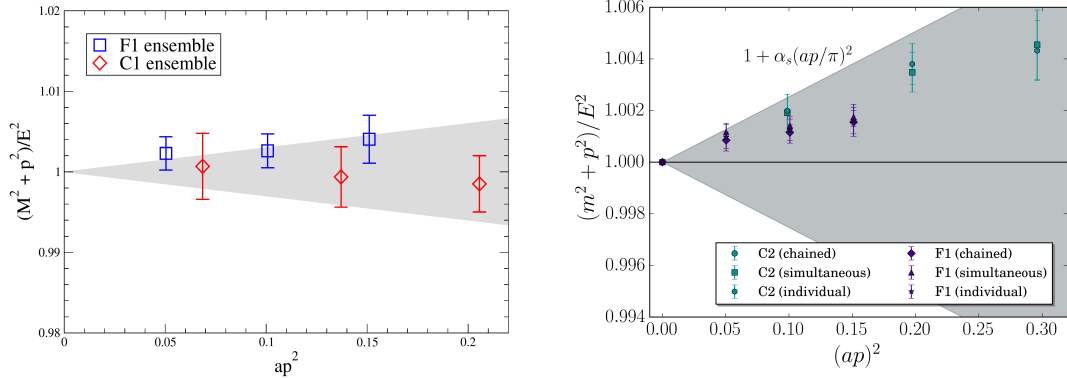
For each ensemble, we determined the ratio $(M_{D_{(s)}}^2 + \vec{p}^2)/E_{D_{(s)}}^2$ and illustrate some results in Figure 1. The shaded region corresponds to $1 \pm \alpha_s (ap/\pi)^2$, where we set $\alpha_s = 0.25$. In contrast to the $B \rightarrow D\ell\nu$ case, the data for the $B_s \rightarrow D_s\ell\nu$ decay lie systematically above the relativistic value of unity, indicating that the statistical uncertainties of the fit results are sufficiently small that we

Table 2: Preliminary results for the form factors, $f_0^{(s)}(\vec{p})$ and $f_+^{(s)}(\vec{p})$. For the $B \rightarrow D\ell\nu$ decay, the results are taken from [8]. From top to bottom, the rows correspond to ensemble sets C1, C2, C3, F1, and F2.

$f_0(0,0,0)$	$f_0(1,0,0)$	$f_0(1,1,0)$	$f_0(1,1,1)$	$f_+(1,0,0)$	$f_+(1,1,0)$	$f_+(1,1,1)$
0.8810(56)	0.8743(43)	0.8608(38)	0.8534(42)	1.135(12)	1.1125(57)	1.0837(61)
0.8809(31)	0.8716(54)	0.8617(44)	0.8503(50)	1.110(12)	1.0809(70)	1.0479(64)
0.8872(23)	0.8685(32)	0.8592(29)	0.8473(38)	1.1282(71)	1.0937(40)	1.0569(50)
0.9034(31)	0.8771(42)	0.8643(41)	0.8479(56)	1.1344(91)	1.0931(59)	1.0480(74)
0.9051(23)	0.8895(36)	0.8702(29)	0.8504(34)	1.1461(72)	1.0963(39)	1.0577(45)
$f_0^s(0,0,0)$	$f_0^s(1,0,0)$	$f_0^s(1,1,0)$	$f_0^s(1,1,1)$	$f_+^s(1,0,0)$	$f_+^s(1,1,0)$	$f_+^s(1,1,1)$
0.8885(11)	0.8754(14)	0.8645(13)	0.8568(13)	1.1384(35)	1.1081(20)	1.0827(21)
0.8822(13)	0.8663(15)	0.8524(16)	0.8418(18)	1.1137(29)	1.0795(22)	1.0470(21)
0.8883(13)	0.8723(16)	0.8603(16)	0.8484(21)	1.1260(34)	1.0912(24)	1.0552(28)
0.9063(10)	0.8848(13)	0.8674(13)	0.8506(17)	1.1453(29)	1.0955(24)	1.0549(24)
0.9047(12)	0.8855(16)	0.8667(15)	0.8487(19)	1.1347(42)	1.0905(26)	1.0457(33)

can resolve discretization effects at $\mathcal{O}(\alpha_s(ap/\pi)^2)$. In both cases, the discretization effects are less than 0.5% in the dispersion relation.

Figure 1: Dispersion relation for the ensemble sets C2 and F1. For the $B_s \rightarrow D_s\ell\nu$ decay (right-hand pane), we include all three types of fits listed in the text (simultaneous, chained, and individual) to illustrate the consistency of our results. The shaded region corresponds to $1 \pm \alpha_s(ap/\pi)^2$ where we take $\alpha_s = 0.25$. The left-hand pane is taken from [8].



We summarize our preliminary results for the form factors, $f_0^{(s)}(\vec{p})$ and $f_+^{(s)}(\vec{p})$, for each ensemble and $D_{(s)}$ momentum, in Table 2.

4. Chiral, continuum and kinematic extrapolations

We express the dependence of the form factors on the z -variable, $z(q^2) = \frac{\sqrt{t_+ - q^2} - \sqrt{t_+ - t_0}}{\sqrt{t_+ - q^2} + \sqrt{t_+ - t_0}}$, where

$t_+ = (M_{B_{(s)}} + M_{D_{(s)}})^2$ and we take $t_0 = q_{\max}^2$, through a modification of the BCL parameterization [14]

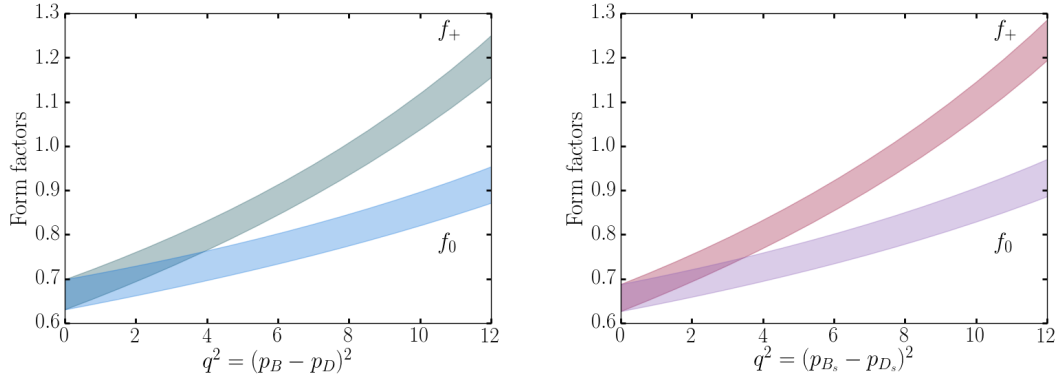
$$f_0^{(s)}(q^2(z)) = \frac{1}{P_0} \sum_{j=0}^{J-1} a_j^{(0,(s))}(m_l, m_l^{\text{sea}}, a) z^j, \quad (4.1)$$

$$f_+^{(s)}(q^2(z)) = \frac{1}{P_+} \sum_{j=0}^{J-1} a_j^{(+,(s))}(m_l, m_l^{\text{sea}}, a) \left[z^j - (-1)^{j-J} \frac{j}{J} z^J \right]. \quad (4.2)$$

Here the $P_{0,+}$ are Blaschke factors that take into account the effects of expected poles above the physical region. The expansion coefficients $a_j^{(0,+,(s))}$ include lattice spacing and light quark mass dependence. We modify this parameterization of the form factors to accommodate the systematic uncertainty associated with the truncation of the matching procedure at $\mathcal{O}(\alpha_s, \Lambda_{\text{QCD}}/m_b, \alpha_s/(am_b))$. We introduce fit parameters m_{\parallel} and m_{\perp} , with central value zero and width $\delta m_{\parallel,\perp}$ and re-scale the form factors, f_{\parallel} and f_{\perp} according to $f_{\parallel,\perp} \rightarrow (1 + m_{\parallel,\perp})f_{\parallel,\perp}$. We take the systematic uncertainties in these fit parameters as 3% and refer the reader to the detailed discussion of this approach in [8].

In Figure 2 we plot our fit results for $f_0^{(s)}(z(q^2))$, $f_+^{(s)}(z(q^2))$ as a function of the momentum transfer, q^2 , for $B \rightarrow D\ell\nu$ (left panel) and $B_s \rightarrow D_s\ell\nu$ (right panel) semileptonic decays. We test the convergence of our fit ansätze by modifying the fit function, as outlined in detail in [8]

Figure 2: Fit results as a function of the momentum transfer, q^2 , for the $B \rightarrow D\ell\nu$ (left) and $B_s \rightarrow D_s\ell\nu$ (right) semileptonic decays. The left-hand pane first appeared, in slightly modified form, in [8].



5. Summary

We have presented lattice calculations of the $B_{(s)} \rightarrow D_{(s)}\ell\nu$ semileptonic decays and determined the form factors, $f_0^{(s)}(q^2)$ and $f_+^{(s)}(q^2)$ over the full kinematic range of momentum transfer. There are currently a number of tensions between experimental measurements and theoretical expectations for semileptonic decays of the B meson. These tensions include the branching fraction ratios, $R(D^{(*)})$, and determinations of $|V_{cb}|$ from exclusive and inclusive decays. Future experimental measurements of semileptonic decays of B_s mesons, in conjunction with our results for the form factors, may provide some insight into these tensions.

The dominant uncertainties in the form factors for the $B_{(s)} \rightarrow D_{(s)}\ell\nu$ decays arise from the discretization effects, with a significant contribution from the matching to full QCD. Higher order

calculations in lattice perturbation theory with the highly improved actions used in this calculation are currently unfeasible, so we are exploring methods to reduce matching errors by combining results calculated using NRQCD with those determined with an entirely relativistic formulation for the b -quark [8, 13].

The LHC is scheduled to significantly improve the statistical uncertainties in experimental measurements of $B_{(s)}$ decays with more data over the next decade. Reduced uncertainties on the corresponding form factors will improve theory errors in the fragmentation function ratio, f_s/f_d , used to extract branching fractions of B_s decays at the LHC, and in determinations of $|V_{cb}|$. These improvements will be necessary to exploit fully the improved statistical precision of future experimental results and ultimately shed light on current tensions in the heavy quark flavor sector.

Acknowledgments

Numerical simulations were carried out on facilities of the USQCD collaboration funded by the Office of Science of the DOE and at the Ohio Supercomputer Center. This work was supported in part by grants from the DOE and NSF. We thank the MILC collaboration for use of their gauge configurations.

References

- [1] LHCb & CMS Collaborations, *Nature* **522** (2015) 68 [1411.4413]
- [2] B. Adeva *et al.*, LHCb collaboration, [0912.4179]
- [3] R. Fleischer, N. Serra and N. Tuning, Niels, *Phys.Rev.D* **82** (2010) 034038 [1004.3982];
R. Fleischer, N. Serra and N. Tuning, Niels, *Phys.Rev.D* **83** (2011) 014017 [1012.2784]
- [4] J. A. Bailey *et al.*, *Phys.Rev.D* **85** (2012) 114502 [1202.6346]
- [5] M. Atoui *et al.*, *Eur.Phys.J.C* **74** (2014) 2861 [1310.5238]
- [6] K.A. Olive *et al.* (Particle Data Group), *Chin.Phys.C* **38** (2014) 090001;
Y. Amhis *et al.* (Heavy Flavor Averaging Group),
[<http://www.slac.stanford.edu/xorg/hfag/semi/index.html>]
- [7] P. Gambino, K. J. Healey and S. Turczyk, (2016) [1606.06174];
D. Bigi and P. Gambino, (2016) [1606.08030]
- [8] H. Na *et al.*, *Phys.Rev.D* **92** (2015) 054510 [1505.03925], [Err.: PRD93 (2016) 119906].
- [9] A. Bazavov *et al.*, *Rev.Mod.Phys.* **82** (2010) 1349 [0903.3598]
- [10] C. J. Monahan, J. Shigemitsu and R. R. Horgan, *Phys.Rev.D* **87** (2013) 034017 [1211.6966]
- [11] H. Na *et al.*, *Phys.Rev.D* **86** (2012) 034506 [1202.4914]
- [12] G. P. Lepage, (2012) [lsqfit v4.8.5.1] and [corrfitter v3.7.1]
- [13] C. M. Bouchard *et al.*, *Phys.Rev.D* **90** (2014) 054506 [1406.2279]
- [14] C. Bourrely, I. Caprini and L. Lellouch, *Phys.Rev.D* **79** (2009) 013008 [0807.2722], [Err.: PRD82 (2010) 099902]